JOURNAL OF FORENSIC SCIENCES

J Forensic Sci, November 2018, Vol. 63, No. 6
doi: 10.1111/1556-4029.13801
Available online at: onlinelibrary.wiley.com

PAPER

ANTHROPOLOGY

Eman Allam,[1,2] *B.D.S., Ph.D.; Philani Mpofu*,[3] *B.A.; Ahmed Ghoneima*,[1,4] *B.D.S., Ph.D., M.S.; Mihran Tuceryan*,[5] *Ph.D.; and Katherine Kula*,[1] *M.S., D.M.D., M.S.*

The Relationship Between Hard Tissue and Soft Tissue Dimensions of the Nose in Children: A 3D Cone Beam Computed Tomography Study

ABSTRACT: This study using three-dimensional cone beam computed tomography (CBCT) images of children determined relationships between nasal skeletal and soft tissue measurements and assessed the association with sex, age, and skeletal maturation stage. Following reliability studies, skeletal and soft tissue parameters were measured on coded CBCTs of 73 children (28M:45F;6–13 yoa). Pearson and Mantel correlations were used to analyze associations between skeletal and soft tissues. Partial Mantel correlations were used to study the associations between skeletal and soft tissue, adjusting for sex, age, and skeletal maturation. Linear regression analyses were used to predict soft tissues sizes. Logistic regression was used to study the relationships between soft and skeletal tissue symmetry. Except for nasal aperture width and interalar width, skeletal landmarks best predicted corresponding soft tissue landmarks. Significant positive associations existed between skeletal and soft tissues after adjusting for sex, skeletal maturation, and age. Children's nasal skeletal tissues predicted nasal soft tissue reasonably well.

KEYWORDS: forensic science, facial reconstruction, nose, children, cone beam computed tomography, predictions

Quantitative analysis of the human face and the ability to reconstruct a person's face from the skeletal remains is of great interest to forensic researchers and anthropologists. The human face shows variations in form and dimensions due to several factors such as genetics, environmental factors, sex, ethnicity, growth, and congenital anomalies (1–3). Facial reconstruction or facial approximation is the process of recreating a face that closely resembles the living individuals from their skulls by rebuilding of the underlying anatomy. The procedure entails predicting a face from the morphology of the skull using mean tissue depth method. The purpose was to assist the identification of the person to whom the remains might belong (4–6).

Nasal morphology is an important feature for facial esthetics and reconstruction as it is considered the most prominent and central structure of the human face. The position, shape, size, and symmetry of the nose are essential determinants of facial expression (7) and attractiveness (8). The nose is composed mostly of cartilage with minimal bone support except for the nasal bone and supporting vomer and maxillary backing. Unfortunately, cartilage decomposes quickly leaving little to build upon for reconstruction purposes. Nasal dimensions significantly affect the facial soft tissue form and the degree of profile convexity. A normal facial morphology requires nasal dimensional harmony with the other features of the face (9–11).

Both processes of facial reconstruction and approximation are relatively successful in identity recognition; however, uncertainty and several problems are still associated with it. Among these problems are the methods available for accurate determination of the relationship between the details of some facial features, including the nose, and the underlying skeletal structures (12–14). Although data for adults are available in the literature (14–16), there are limited data available for children (17–19). Most of these data are from lateral cephalograms which limit frontal information.

Although some research suggests that the facial form and dimensions are not exclusively defined by the underlying skeletal tissues, the relationship between skeletal and soft tissue parameters could provide valuable information about the strength of correlation and the accuracy of the prediction process. The purpose of this retrospective study was to determine the relationship between skeletal and soft tissue measurements of the nose using three-dimensional cone beam computed tomography (3D CBCT) images in a sample of children 6–13 years old as well as to assess the degree of association with sex, chronological age, and skeletal maturation stage.

Materials and Methods

Seventy-three pre-orthodontic treatment CBCTs for Caucasian children (28 males and 45 females) aged 6–13 years were

[1]Department of Orthodontics and Oral Facial Genetics, Indiana University School of Dentistry, Indianapolis, IN.
[2]Oral and Dental Research Division, National Research Centre, Cairo, Egypt.
[3]Department of Biostatistics, Indiana University School of Medicine, Indianapolis, IN.
[4]Department of Orthodontics, Hamdan Bin Mohammed College of Dental Medicine, Dubai, UAE.
[5]Department of Computer Sciences, Indiana University, Indianapolis, IN.
Corresponding author: Katherine Kula, M.S., D.M.D., M.S. E-mail: kkula@iu.edu

[This article was published online on 23 April 2018. Errors were subsequently identified in the author affiliations. The article was corrected on 31 July 2018.]

Received 19 Dec. 2017; and in revised form 21 Feb. 2018; accepted 5 Mar. 2018.

retrieved from the archives of the Orthodontic Department at Indiana University School of Dentistry. The study was approved by the university institutional review board committee. Subjects with severe facial asymmetry or any form of systemic diseases or craniofacial abnormality, facial surgery or rhinoplasty were excluded. All CBCTs were taken with the same i-CAT CBCT (Imaging Sciences, Hatfield, PA) set for full 13 cm field of view, 20 sec of scanning time, and a resolution of 0.4 mm voxel size. The CBCT data were exported in Digital Imaging and Communications in Medicine (DICOM) format, and Dolphin Imaging software, version 11.7 (Dolphin Imaging, Chatsworth, CA) was used for all analysis. Threshold level of the constructed 3D imaging was set and standardized for each structure using the software rendering segmentation feature of bone and soft tissue structures. Soft tissue segmentation was performed by adjusting the range of the lower and upper density boundaries between the patient's air and soft tissue with HU range of −520 to 500, while hard tissue was segmented by adjusting the lower and upper density boundaries between the patient's soft tissue and hard tissue with HU range of 500–1100. All 3D CBCT images were oriented in the sagittal, axial, and coronal planes before taking measurements. Orientation process was performed using the same software by adjusting the midsagittal plane with the skeletal midline of the face, the axial plane with the Frankfort horizontal plane, and coronal plane passing through the apex of the zygomatic bone.

Soft tissue landmarks: (Pn) pronasale; (Al) alare; (Sn) subnasale; and (N′) soft tissue nasion as well as skeletal landmarks: (N) nasion; (Rh) rhinion; (NC) nasal aperture; and (ANS) anterior nasal spine were identified and located. Skeletal and soft tissue parameters (Table 1 and Figs 1–4) were measured on all coded constructed 3D CBCT images for both soft tissue and skeletal structures. Skeletal measurements included the following: nasal length (N-ANS, N-Rh), nasal aperture width, medial interorbital distance, lateral interorbital distance, surface area of the NC, nasofrontal angle, and symmetry. Soft tissue measurements included the following: nasal length (N′-Sn), interalar distance, inner canthal distance, outer canthal distance, size of the nose, nasofrontal angle, and symmetry. Symmetry was determined by assessing balance or equal sections (within 10% difference) on opposite sides of a constructed midsagittal plane.

The skeletal age of the included sample was assessed and classified into five stages according to the cervical vertebral maturation (CVMS) method (20). The five stages of CVMS were determined according to the maturation changes seen in shape and size of the second, third, and fourth cervical vertebrae. All data were collected by one investigator who was blinded to the identity of the coded images. Prior to data collection, intrarater reliability was assessed by repeating all measurements twice 2 weeks apart by the same investigator on 10 randomly selected cases. In order to allow the investigator to continue with data collection, the intraclass correlation coefficient (ICC) was considered acceptable reliability if $r \geq 0.90$.

Statistical Methods

All ICC values were greater than 0.90. The sample mean ages (SD) for males and females were 10.62(1.69) and 10.31(1.96) years, respectively. A two-sample at the 0.05 alpha level suggests no evidence of a difference in mean age with respect to sex ($t = -0.711$, DF = 63.708, p-value = 0.4798).

All skeletal measurements were considered the predictor variables, while soft tissue measurements were the response variables. Each soft tissue measurement was paired with a skeletal tissue measurement with the goal of studying how well the skeletal measure can act as a surrogate/predictor of the soft tissue measure. Skeletal measures considered included the following: nasal length (N-ANS), nasal length (N-Rh), nasal aperture width, medial interorbital distance, lateral interorbital distance, surface area of the nasal aperture, nasofrontal angle (skeletal), and symmetry [1-Yes, 0-No]. The soft tissue measurements included the following: nasal length (N′-Sn), nasal length (N′-Sn), interalar distance, inner canthal distance, outer canthal distance, nose size, nasofrontal angle (soft tissue), and symmetry [1-Yes, 0-No]. The specific pairings of soft and hard tissue characteristics were paired.

Sample mean and standard deviation were computed for continuous variables, and frequencies were computed for categorical variables. Pearson correlations were computed for continuous soft and hard tissue pairings as defined before. Logistic regression was used to study the relationship between symmetry at soft and hard tissue levels. Prediction of soft tissue feature based on corresponding hard tissue feature was performed using simple linear regression. Predictions and prediction intervals were obtained based on leave-one-cross-validation (LOOCV). Based on data, under the assumption of linear relationships between soft at hard tissues features, the prediction equations were are follows:

$$\widehat{\text{Nasal length}}\,(\text{N}' - \text{Sn}) = 25.288 + 0.372 \times \text{Nasal length}\,(\text{N} - \text{ANS})$$

$$\widehat{\text{Nasal length}}\,(\text{N}' - \text{Sn}) = 36.22 + 0.317 \times \text{Nasal length}\,(\text{N} - \text{Rh})$$

$$\widehat{\text{Interalar distance}} = 34.512 - 0.172 \times \text{Nasal aperture width}$$

TABLE 1—*Skeletal and soft tissue nose measurements.*

Measurement	Definition
Skeletal	
Nasal length (two different measures)	Distance between nasion (N) to anterior nasal spine (ANS) or to rhinion (Rh)
Nasal aperture width	Distance between left and right lateral piriform rims
Medial interorbital distance	Distance between the medial walls of the bony orbits
Lateral interorbital distance	Distance between the lateral walls of the bony orbits
Surface area of the nasal aperture	Surface area of the air-filled space outlined by the bony walls
Nasofrontal angle	Angle formed by the intersection of the nasion (N) with lines tangent to the glabella and rhinion (Rh)
Soft tissue	
Nasal length	Distance between soft tissue nasion (N′) and subnasale (Sn)
Interalar distance	Distance between the outer points of the ala of the nose in a straight line corresponding to the nose width
Inner canthal distance	Distance between the medial angles of the palpebral fissures
Outer canthal distance	Distance between the lateral margins of the eyes
Size of the nose	Area measured from bridge of the nose and outlining the nose
Nasofrontal angle	Angle formed by the intersection of the nasion (N′) with lines tangent to the glabella and pronasale (Pn)

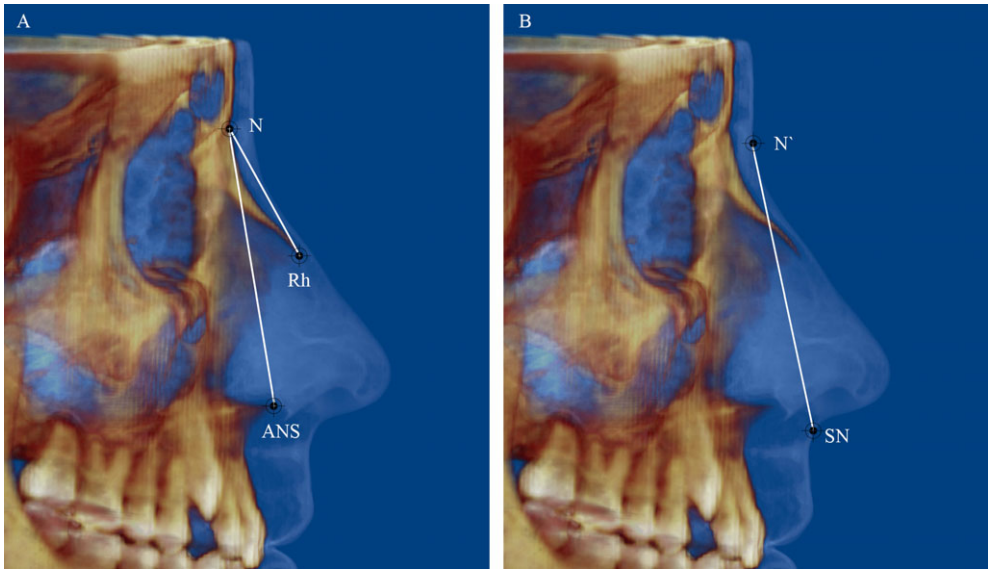

FIG. 1—*3D CBCT reconstructed image showing skeletal (A) and soft tissue (B) nasal length. [Color figure can be viewed at wileyonlinelibrary.com]*

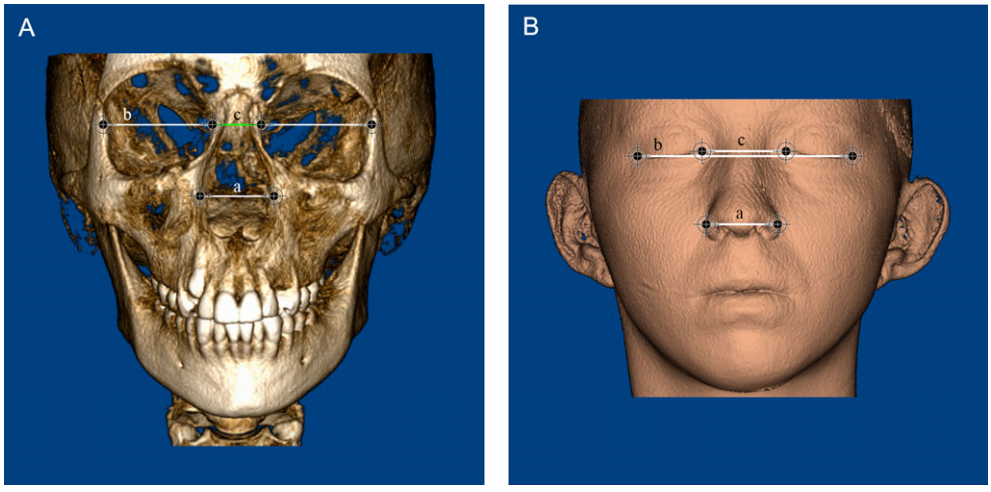

FIG. 2—*3D CBCT image showing A: skeletal measurements of a) nasal aperture width, b) lateral interorbital distance, c) medial interorbital distance and B: soft tissue measurements of a) interalar distance, b) outer canthal distance, and c) inner canthal distance. [Color figure can be viewed at wileyonlinelibrary.com]*

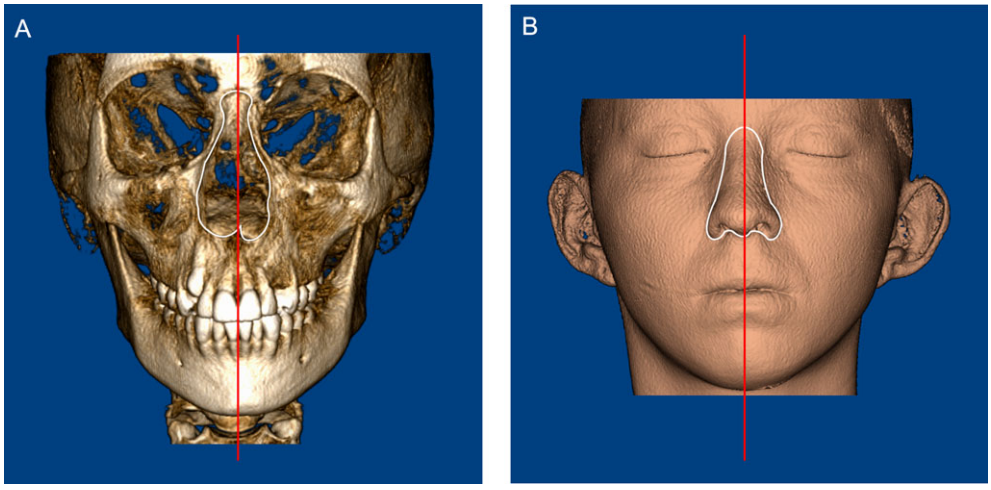

FIG. 3—*3D CBCT image showing A: skeletal surface area of the nasal aperture and nasal symmetry, B: soft tissue surface area of the nose and nasal symmetry. [Color figure can be viewed at wileyonlinelibrary.com]*

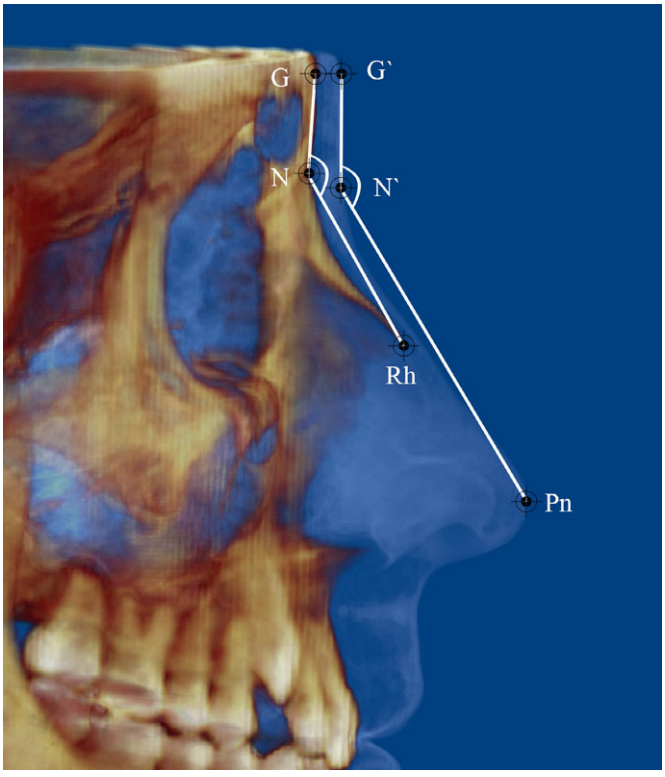

FIG. 4—*3D CBCT image showing the a) skeletal and b) soft tissue nasofrontal angle. [Color figure can be viewed at wileyonlinelibrary.com]*

$$\text{Inner canthal distance} = 21.249 + 0.456 \times \text{Medial interorbital distance}$$

$$\text{Outer canthal distance} = 17.947 + 0.769 \times \text{Lateral interorbital distance}$$

$$\text{Nose Size} = 63.529 + 0.66 \times \text{Surface area of the nasal aperature}$$

$$\text{Nasofrontal angle} = 93.28 + 0.371 \times \text{Nasofrontal angle (skeletal)}$$

We also studied the simultaneous association between soft and hard tissue features. To allow for simultaneous analysis, exploratory and response variables were packaged in matrices. We called the matrix of explanatory variables $\boldsymbol{X}$, and that of response variables $\boldsymbol{Y}$.

Correlation between matrices of soft and hard tissue measurements was assessed using the Mantel test. This method was appealing because response and explanatory matrices contained mixtures data types. In particular, variables under consideration are continuous, nominal, or ordinal. To perform the Mantel test, the matrices of soft ($\boldsymbol{Y}$) and hard ($\boldsymbol{X}$) tissue measurements were converted into Euclidean distance matrices. This conversion allowed us to answer this question: "If two hard tissue measurements (x_i, x_j) are similar does that also mean the corresponding soft tissue measures (y_i, y_j) are similar?" Subgroup analyses were performed to assess Mantel correlations when observations were stratified by sex (male, female), age (6–10, >10 years), and skeletal maturation (CVMS: 1–3, 4–6). Partial Mantel test was performed to assess correlation after adjusting for sex, age, and skeletal maturation. All statistical tests were performed at the 0.05 alpha level. Analyses were performed using R version 3.4.1 (21–24).

Results

Descriptive statistics and patients' characteristics are described in Table 2. The Pearson correlations between the soft and hard tissue pairings are presented in Table 3.

For the most part, the correlations between the pairings were positive and statistically significant, except for the correlation between nasal aperture width and interalar distance, which was negative and not statistically significant at the 0.05 alpha level. The pairwise associations ranged from weak to moderate strength. Logistic model suggested that the odds of having symmetric soft features among those with symmetric hard features were approximately 14 times the odds of having symmetric soft features among those with nonsymmetric hard features (95% C.I.: (2.91–65.25)). This odds ratio suggests a very strong relationship between symmetry at skeletal and soft tissue levels.

In simultaneous analysis of association using partial Mantel test, we found a positive association between soft and hard tissue features while adjusting for sex, skeletal maturation, and age (p-value = 0.0001; Table 4). Sex and skeletal maturation (based on CVMS) showed significant correlations with nasal hard and soft tissue size (Table 4). The group over 10 years of age also showed significant correlations with nasal size, whereas the age group 6–10 years only approached significance.

Based on simple linear regression model, we obtained predictions and 95% prediction intervals for a random sample of 10 subjects. The predictions are presented in Table 5. Many of the predicted values were within a mm of the actual values of the subjects. The subjects with the greatest differences varied as shown by the bolding for each measure. Bivariate plots showing the relationships between correlated soft and hard tissue features are shown in Fig. 5. Each plot consists of estimated mean response, 95% point-wise confidence band, and 95% point-wise prediction band. Mean response represented by solid black line; 95% point-wise confidence interval is represented by gray shaded area; and, 95% point-wise prediction band is represented by dashed black lines.

Discussion

The external nose is a complex anatomical structure that is considered specifically critical for the process of facial reconstruction and predicting facial morphology of an individual from unknown skeletal remains. Although both skeletal and soft tissue structures affect the facial balance and form, most of the visual impact of the face is provided by the structure of the overlying soft tissue and their relative dimensions and proportions (25,26). At the same time, for forensic and anthropology research dealing with facial reconstruction purposes, only skeletal remnants are available in most cases. For this reason, studying the relationship and degree of association is particularly important. In the current retrospective study, CBCT images were used to assess the relationship between skeletal and soft tissue measurements of the nose in a sample of 6- to 13-year-old children as well as to determine the degree of association with sex, chronological age, and skeletal maturation stage. CBCT is an important tool for 3D evaluation of craniofacial anatomical structures. It provides clinicians with opportunity for 3D volumetric renderings and allows accurate quantification of measurements. It is also considered particularly valuable in assessing the relationship between hard and soft tissues of the maxillofacial region (27,28).

TABLE 2—*Sample characteristics and descriptive statistics of skeletal and soft tissue measures.*

		Sex		Age Group		CVMS		
	Overall (N = 73)	Female (N = 45)	Male (N = 28)	6–10 (N = 24)	>10 (N = 49)	1–2 (N = 44)	3–4 (N = 26)	5 (N = 3)
Skeletal, mean(SD)								
Nasal length (N-ANS, mm)	44.5 (3.64)	44.7 (3.74)	44.1 (3.52)	44.1 (4.62)	44.7 (3.1)	44.2 (3.72)	44.6 (3.37)	47.4 (4.94)
Nasal length (N-Rh, mm)	17.8 (3.14)	17.7 (3.52)	18.0 (2.45)	18.0 (3.08)	17.7 (3.19)	17.5 (2.36)	18.2 (4.03)	19.0 (5)
Nasal aperture width (mm)	22.1 (1.56)	22.0 (1.26)	22.3 (1.96)	21.7 (1.46)	22.3 (1.58)	22.1 (1.48)	22.0 (1.47)	24.2 (2.51)
Medial interorbital distance (mm)	17.1 (2.16)	16.9 (2.34)	17.3 (1.84)	17.6 (2.26)	16.8 (2.08)	17.5 (2.21)	16.4 (2.03)	16.1 (0.7)
Lateral interorbital distance (mm)	86.2 (3.9)	85.3 (3.37)	87.8 (4.24)	85.9 (4.35)	86.4 (3.7)	86.2 (4.2)	86.4 (3.29)	84.9 (5.64)
Surface area of the nasal aperture (mm)	107.1 (12.04)	108.5 (12.7)	104.9 (10.73)	106.5 (13.14)	107.4 (11.59)	106.2 (10.97)	107.4 (13.11)	116.9 (17.91)
Nasofrontal angle (°)	143.5 (8.31)	144.3 (7.98)	142.2 (8.81)	143.5 (7.93)	143.5 (8.57)	144.8 (8.87)	140.7 (6.82)	148.4 (6.34)
Symmetry								
No, n(%)	36 (49.3)	23 (51.1)	13 (46.4)	14 (58.3)	22 (44.9)	20 (45.5)	15 (57.7)	1 (33.3)
Yes, n(%)	37 (50.7)	22 (48.9)	15 (53.6)	10 (41.7)	27 (55.1)	24 (54.5)	11 (42.3)	2 (66.7)
Soft tissue, mean(SD)								
Nasal length (N′-Sn, mm)	41.9 (3.25)	41.8 (3.34)	41.9 (3.17)	41.6 (3.43)	42.0 (3.19)	41.8 (2.83)	41.3 (3.51)	47.3 (2.26)
Interalar distance (mm)	30.7 (1.96)	30.1 (1.84)	31.7 (1.76)	30.9 (1.84)	30.6 (2.03)	30.8 (2.17)	30.6 (1.65)	29.8 (1.31)
Inner canthal distance (mm)	29.0 (2.97)	28.7 (2.94)	29.5 (3)	29.1 (3.84)	29.0 (2.48)	29.1 (3.14)	29.0 (2.77)	29.0 (3.1)
Outer canthal distance (mm)	84.3 (4.31)	83.7 (3.7)	85.2 (5.09)	84.0 (4.77)	84.4 (4.12)	84.1 (4.43)	84.6 (4.29)	83.7 (4.11)
Nose size (mm)	134.2 (12.87)	135.5 (13.59)	132.2 (11.55)	135.2 (13.75)	133.8 (12.53)	132.9 (11.62)	136.3 (15.21)	136.1 (8.37)
Nasofrontal angle (°)	146.6 (6.29)	147.0 (6.11)	145.9 (6.63)	145.2 (5.43)	147.3 (6.62)	146.4 (6.41)	146.2 (5.77)	152.8 (8.05)
Symmetry								
No, n(%)	18 (24.7)	12 (26.7)	6 (21.4)	4 (16.7)	14 (28.6)	6 (13.6)	11 (42.3)	1 (33.3)
Yes, n(%)	55 (75.3)	33 (73.3)	22 (78.6)	20 (83.3)	35 (71.4)	38 (86.4)	15 (57.7)	2 (66.7)

TABLE 3—*Pearson correlations of skeletal and overlying soft tissue parameters.*

Skeletal Parameter	Soft Tissue Parameter	Correlation	t	p-value*
Nasal length (N-ANS)	Nasal length (N′-Sn)	0.42	3.87	0.000
Nasal length (N-Rh)	Nasal length (N′-Sn)	0.31	2.71	0.009
Nasal aperture width	Interalar distance	−0.14	−1.16	0.248
Medial interorbital distance	Inner canthal distance	0.33	2.96	0.004
Lateral interorbital distance	Outer canthal distance	0.70	8.16	0.000
Nasal aperture surface area	Nose size	0.62	6.62	0.000
Nasofrontal angle (skeletal)	Nasofrontal angle (soft tissue)	0.49	4.74	0.000

*$p \leq 0.05$ accepted as significant.

TABLE 4—*Statistical correlations between soft and hard tissue measures.*

Variable	N	Mantel Correlation	p-value*
(Y vs. X)	73	0.392	0.0001
Adjusted*	73	0.388	0.0001
Sex			
Female	45	0.349	0.0002
Male	28	0.570	0.0001
Skeletal maturation			
CVMS: 1–2	44	0.464	0.0001
CVMS: 3–4	26	0.274	0.0177
Age			
Age: 6–10	24	0.254	0.0523
Age: >10	49	0.466	0.0001

*Partial Mantel test: Adjusting for sex, skeletal maturation, and age grouping. Mantel test- $p \leq 0.05$ accepted as significant.

The present study showed that, in general, there is a weak to moderate positive relationship between nasal soft and hard tissue measures and that this positive relationship is maintained with stratified analyses of sex, age, and skeletal maturation. The correlation analysis results suggested that skeletal parameters such as the nasal length, medial and lateral interorbital distance, surface area of the nasal aperture, symmetry, and nasofrontal angle are the strongest positive determinants of their corresponding soft tissue parameters with the nasal aperture width and interalar distance being the exception. These findings provide strong evidence that it is possible, in children, using appropriate facial approximation methods, to predict the form of the external nose from the skeletal tissues.

In agreement with these findings, Inada et al. (29) investigated the relationship between nasal and skeletal landmarks on lateral cephalograms in preschool children. A stepwise regression analysis was used to determine how combinations of skeletal landmarks might explain nasal form. They found that the soft tissue nasal landmarks can be reliably predicted from selected skeletal landmarks. Lee et al. (18) reported that hard and soft tissue relation data from CBCT can be useful for predicting the position of the adult nose. Their results indicated that the anteroposterior, mediolateral, and inferosuperior positions of pronasale, subnasale, and ala were significantly correlated with the measurements of nasal bone and nasal aperture and that regression models for the position of the nose can be determined from the measurements of nasal bone and nasal aperture.

TABLE 5—*Predictions applied to nasal measures of 10 randomly selected subjects. Bolding indicates the greatest difference(s) between observed and predicted measures.*

Skeletal Parameter (*X*)	Soft Tissue Parameter (*Y*)	Subject	Actual	Predicted	95% Prediction Interval	
					Lower	Upper
Nasal length (N-ANS)	Nasal length (N′-Sn)	8	45.6	42.11	36.16	48.07
		21	**46.7**	**42.09**	**36.14**	**48.05**
		27	44.2	43.71	37.68	49.73
		42	42.6	43.65	37.63	49.67
		30	42.4	42.8	36.83	48.77
		62	45.3	40.3	34.31	46.3
		6	46.9	41.72	35.76	47.67
		52	39.6	41.48	35.52	47.44
		3	42.9	41.24	35.28	47.2
		61	46	41.19	35.23	47.15
Nasal length (N-Rh)	Nasal length (N′-Sn)	8	45.6	42.8	36.49	49.1
		21	46.7	41.53	35.27	47.79
		27	44.2	42.99	36.67	49.31
		42	42.6	41.13	34.85	47.41
		30	42.4	42.08	35.82	48.34
		62	45.3	40.9	34.61	47.19
		6	**46.9**	**41.69**	**35.43**	**47.95**
		52	39.6	41.38	35.11	47.66
		3	42.9	40.75	34.45	47.06
		61	**46**	**40.7**	**34.39**	**47**
Nasal aperture width	Interalar distance	8	32	30.64	26.75	34.54
		21	32.1	30.84	26.94	34.75
		27	31.8	31.01	27.08	34.95
		42	30	30.47	26.55	34.39
		30	30.9	31.27	27.27	35.27
		62	31.8	30.92	27	34.83
		6	30.3	30.74	26.84	34.63
		52	**27.6**	**30.6**	**26.69**	**34.51**
		3	30.5	30.65	26.75	34.54
		61	29.9	30.83	26.93	34.73
Medial interorbital distance	Inner canthal distance	**8**	**34.1**	**30.01**	**24.27**	**35.75**
		21	27.2	29.64	23.93	35.34
		27	30.6	30.13	24.38	35.87
		42	29.6	29.92	24.2	35.64
		30	28.4	28.64	22.94	34.34
		62	30.7	27.17	21.37	32.97
		6	31.9	28.87	23.18	34.56
		52	27.6	28.88	23.19	34.58
		3	27.7	29.25	23.56	34.94
		61	26.2	28.14	22.41	33.87
Lateral interorbital distance	Outer canthal distance	8	88.9	90.31	83.9	96.73
		21	92.8	90.18	83.76	96.6
		27	82.7	82.37	76.11	88.63
		42	84.9	86.48	80.22	92.75
		30	83.9	83.6	77.36	89.85
		62	**77.5**	**84.47**	**78.23**	**90.72**
		6	84.6	85.31	79.06	91.56
		52	85.5	81.59	75.32	87.87
		3	85.2	84.68	78.43	90.92
		61	81.8	82.78	76.52	89.03
Surface area of the nasal aperture	Nose size	8	148.6	155.59	134.26	176.92
		21	123.9	128.66	108.18	149.15
		27	157.7	152.31	131.15	173.47
		42	128.6	135.33	114.91	155.74
		30	156.3	152.38	131.22	173.54
		62	126.7	129.21	108.74	149.68
		6	131.4	144.32	123.7	164.94
		52	122	130.03	109.57	150.48
		3	**163.5**	**139.74**	**119.24**	**160.23**
		61	133.5	131.1	110.67	151.54

Prediction of nasal dimensions has been controversial. As early as in 1955, Gerasimov (30) proposed that "the soft part of the nose is a natural continuation of the bony part" and that prediction of the nasal form could be possible using a simple "two-tangent" illustration method. This method entails drawing a line between the bony nasion and prosthion (the most anterior part of maxillary alveolar bone), and a parallel line touching rhinion. He then mirrored the lateral border of the piriform

TABLE 5—*Continued.*

Skeletal Parameter (*X*)	Soft Tissue Parameter (*Y*)	Subject	Actual	Predicted	95% Prediction Interval	
					Lower	Upper
Nasofrontal angle (skeletal)	Nasofrontal angle (soft tissue)	8	150.5	150.96	139.78	162.13
		21	**132.5**	**143.65**	**132.54**	**154.75**
		27	148.5	147.58	136.55	158.61
		42	151	150.13	139.01	161.25
		30	152.4	145.94	134.92	156.97
		62	145.7	146.53	135.5	157.55
		6	147.6	148.24	137.19	159.28
		52	148.1	143.62	132.53	154.7
		3	149	148.02	136.98	159.06
		61	143.5	148.43	137.38	159.47

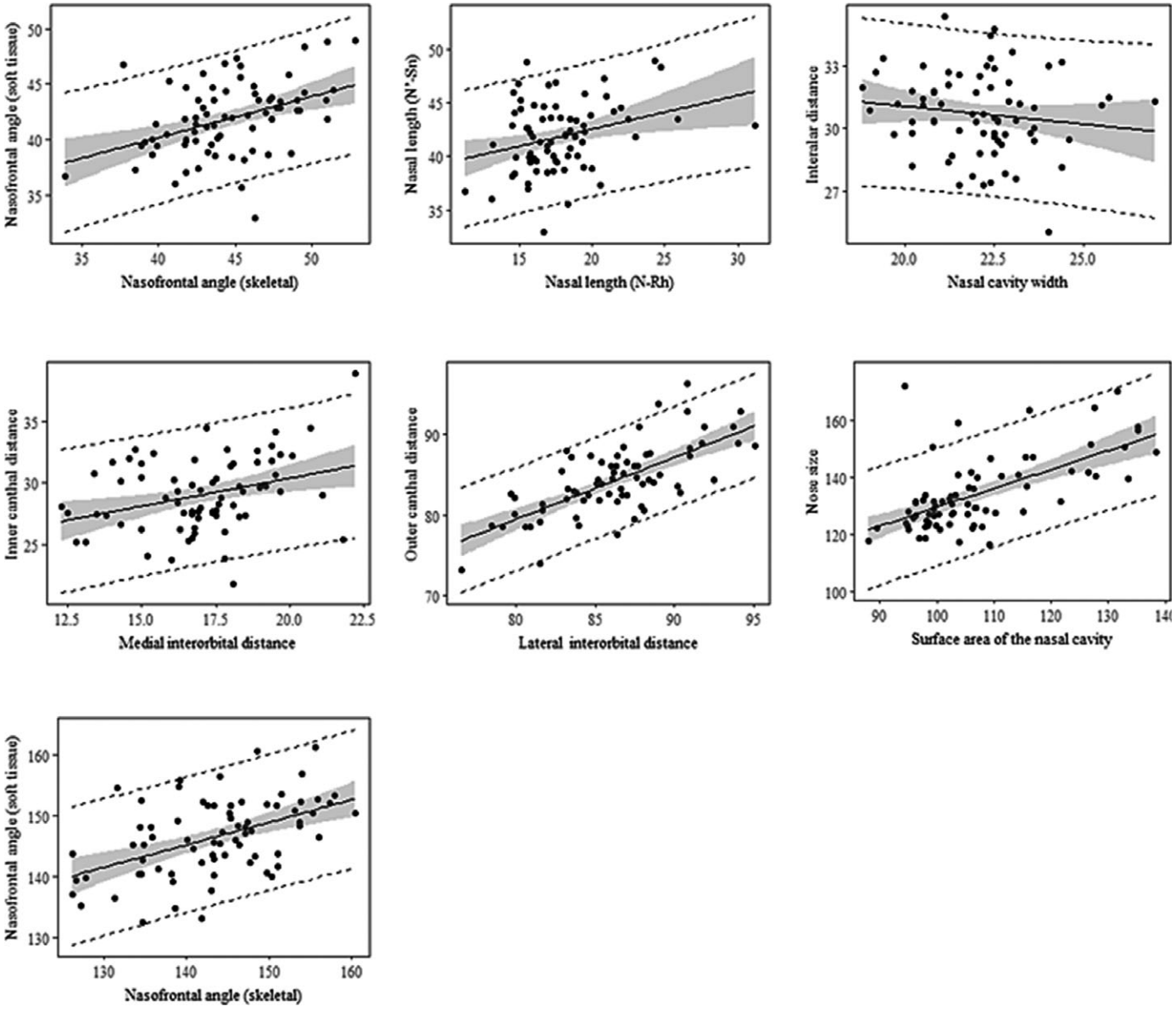

FIG. 5—*Bivariate plot showing the relationships between soft and hard tissue features. Each plot consists of estimated mean response (solid black line), 95% point-wise confidence band (gray shaded area), and 95% point-wise prediction band (dashed black lines).*

aperture about this line by way of projected perpendiculars of equal length on either side. He suggested that this illustrated the profile of the nasal cartilage and so added 2 mm to account for the skin depth. In 2003, Stephan et al. (13) concluded that this method was not reliable at predicting pronasale projection when tested on 59 lateral cephalograms. In a later study, Rynn and Wilkinson (4) tested six methods of predicting external nasal profile proportions, using the form and dimensions of the bony nasal aperture. They suggested that the most useful and practical method of nose and nasal tip prediction was the two-tangent method.

The results of our current study also showed that the observed correlation for males was higher than that of females. This finding could possibly be explained by the fact that boys have greater skeletal measures, thicker soft tissues, and larger increments in nasal dimensions than girls (13,31). However, there is disagreement between these results and previous literature demonstrating that there are no sex differences in nasal soft and hard tissues dimensions and relations. The study conducted by Djupesland and Lyholm (32) indicated that the size of the nose and the airspace in the nasal aperture did not depend upon the sex. Likus et al. (33) reported the absence of statistically significant differences between the sexes, as regards the values and relations of all nasal parameters measured. The disagreement between findings could be explained by the differences in the age of the studied samples. Most of these studies were performed on adult populations, while in our study, the sample consisted of growing children where maturational changes and growth rates are considered critical factors and well known to be different, at certain points, between both sexes.

When applying stratified analysis of age, results suggested a difference in correlation among subjects aged 6–10 and those older than 10 years. Correlation observed for subjects older than 10 years group was stronger than that in the 6–10 age group. This could be possibly explained by the fact that the greatest amount of changes related to vertical growth in the craniofacial region and the growth spurt usually occurs in children older than 10 years. More changes associated with pubertal spurts and more vertical growth of the maxilla are expected in children at age 10–13 years. Subtelny (34) reported that a spurt was seen in a male's nasal growth from 10 to 16 years with a peak around 13–14 years. He also verified that in subjects whose total growth pattern did not show spurt characteristics, the configuration of the profile of the nose seemed to maintain itself with progressing age. In the majority of boys and in few girls when a growth spurt was evident, there were some concomitant changes in the relationship of the nasal bone to other cranial bones. Heijden et al. (35) indicated that the average age of maturity is 13.4 years for girls and 14.7 years for boys, while nasal growth velocity is maximal at the mean (SD) age of 11.0 (0.9) years for girls and 12.6 (0.3) years for boys. In the current study, for age and skeletal maturation stratified analysis, at all levels, a positive correlation between hard and soft tissues measurements was reported. This indicates that nasal form and dimensional changes are affected with chronological age and the maturity level as well as the individual skeletal maturity.

Sforza et al. (15) studied age- and sex-related changes in the external nose in a sample of patients aged 4–73 years dividing them into 11 nonoverlapping age groups. They reported that, on average, men had larger nasal external volume and area, linear distances, and nasal width-to-height ratio than women and that age significantly influenced all analyzed nose measurements. Nasal volume, area, linear distances increased from childhood to old age, while the nasal tip angle decreased as a function of age. Macho (36) demonstrated that the height and the length of the nose were relatively predictable on the basis of several measurements taken from the skull and that the nasal depth and the thickness of the soft tissue were greatly influenced by age.

In conclusion, the results of the present study suggested that, in growing children, nasal soft tissue dimensions could be predictable based on corresponding skeletal measurements and that hard and soft tissue relation data of the nose are useful reference for the facial reconstruction purposes. It is also suggested that, when proposing relationship between nasal soft tissues and bone anatomy, it is important to determine the growth status and potential of the child and whether or not the pubertal growth spurt has been reached.

Acknowledgments

Funding was made available through the Jarabak Endowed Professorship within the Indiana University Foundation.

References

1. Sforza C, de Menezes M, Ferrario VF. Soft-and hard-tissue facial anthropometry in three dimensions: what's new. J Anthropol Sci 2013;91:159–84.
2. Gatliff BP. Facial sculpture on the skull for identification. Am J Forensic Med Pathol 1984;5(4):327–32.
3. Taylor KTT. Forensic art and illustration. Boca Raton, FL: CRC Press, 2001.
4. Rynn C, Wilkinson CM. Appraisal of traditional and recently proposed relationships between the hard and soft dimensions of the nose in profile. Am J Phys Anthropol 2006;130(3):364–73.
5. Wilkinson C. Computerized forensic facial reconstruction: s review of current systems. Forensic Sci Med Pathol 2005;1(3):173–7.
6. Berar M, Tilotta FM, Glaunès JA, Rozenholc Y. Craniofacial reconstruction as a prediction problem using a Latent Root Regression model. Forensic Sci Int 2011;210(1–3):228–36.
7. Pochedly JT, Widen SC, Russell JA. What emotion does the "facial expression of disgust" express? Emotion 2012;12(6):1315–9.
8. Roxbury C, Ishii M, Godoy A, Papel I, Byrne PJ, Boahene KDO, et al. Impact of crooked nose rhinoplasty on observer perceptions of attractiveness. Laryngoscope 2012;122(4):773–8.
9. Schendel SA, Carlotti AE. Nasal considerations in orthognathic surgery. Am J Orthod Dentofacial Orthop 1991;100(3):197–208.
10. Czamecki ST, Nanda RS, Currier GF. Perceptions of a balanced facial profile. Am J Orthod Dentofacial Orthop 1993;104(2):180–7.
11. Gruber RP, Peck GC. Rhinoplasty: state of the art. St Louis, MO: Mosby, 1993.
12. Vanezis M, Vanezis P. Cranio-facial reconstruction in forensic identification – historical development and a review of current practice. Med Sci Law 2000;40(3):197–205.
13. Stephan CN, Henneberg M, Sampson W. Predicting nose projection and pronasale position in facial approximation: a test of published methods and proposal of new guidelines. Am J Phys Anthropol 2003;122(3):240–50.
14. Simpson E, Henneberg M. Variation in soft-tissue thicknesses on the human face and their relation to craniometric dimensions. Am J Phys Anthropol 2002;118(2):121–33.
15. Sforza C, Grandi G, De Menezes M, Tartaglia GM, Ferrario VF. Age- and sex-related changes in the normal human external nose. Forensic Sci Int 2011;204(1-3):205.e1–e9.
16. Tedeschi-Oliveira SV, Beaini TL, Melani RF. Forensic facial recognition: nasal projection in Brazilian adults. Forensic Sci Int 2016;266:123–9.
17. Utsuno H, Kageyama T, Uchida K, Kibayahi K, Sakurada K, Uemura K. Pilot study to establish a nasal tip prediction method from unknown human skeletal remains for facial reconstruction and skull photo superimposition as applied to a Japanese male populations. J Forensic Legal Med 2016;38:75–80.

18. Lee KM, Lee WJ, Cho JH, Hwang HS. Three-dimensional prediction of the nose for facial reconstruction using cone-beam computed tomography. Forensic Sci Int 2014;236:194.e1–5.
19. Peckmann TR, Manhein MH, Listi GA, Fournier M. *In vivo* facial tissue depth for Canadian aboriginal children: a case study from Nova Scotia, Canada. J Forensic Sci 2013;58(6):1429–38.
20. Franchi L, Baccetti T, McNamara JA. Mandibular growth as related to cervical vertebral maturation and body height. Am J Orthod Dentofacial Orthoped 2000;118(3):335–40.
21. Legendre P, Fortin MJ. Spatial pattern and ecological analysis. Vegetatio 1989;80(2):107–38.
22. Abdi H, Williams LJ. Partial least squares methods: partial least squares correlation and partial least square regression. Methods Mol Biol 2013;930:549–79.
23. Chessel D, Dufour AB, Dray S. Analysis of ecological data: exploratory and euclidean methods in environmental sciences. Ver 1.4-14.2 2010;1:4; https://cran.r-project.org/web/packages/ade4/index.html. Accessed March 30, 2018.
24. Mevik BH, Wehrens R. The pls package: principal component and partial least squares regression in R. J Stat Softw 2007;18(2):1–23.
25. Gulsen A, Okay C, Aslan BI, Uner O, Yavuzer R. The relationship between craniofacial structures and the nose in Anatolian Turkish adults: a cephalometric evaluation. Am J Orthodont Dentofacial Orthop 2006;130(2):131.e15–e25.
26. Ferrario VF, Sforza C. Size and shape of soft-tissue facial profile: effects of age, gender, and skeletal class. Cleft Palate Craniofac J 1997;34 (6):498–504.
27. Ghoneima A, Kula K. Accuracy and reliability of cone-beam computed tomography for airway volume analysis. Eur J Orthod 2013;35(2):256–61.
28. Fourie Z, Damstra J, Gerrits PO, Ren Y. Accuracy and repeatability of anthropometric facial measurements using cone beam computed tomography. Cleft Palate Craniofac J 2011;48(5):623–30.
29. Inada E, Saitoh I, Hayasaki H, Iwase Y, Kubota N, Tokemoto Y, et al. Relationship of nasal and skeletal landmarks in lateral cephalograms of preschool children. Forensic Sci Int 2009;191:111.e1–4.
30. Gerasimov MM. The face finder. New York, NY: CRC Press, 1971.
31. Samoliński BK, Grzanka A, Gotlib T. Changes in nasal cavity dimensions in children and adults by gender and age. Laryngoscope 2007;117 (8):1429–33.
32. Djupesland PG, Lyholm B. Changes in nasal airway dimensions in infancy. Acta OtoLaryngolog 1998;118(6):852–8.
33. Likus W, Bajor G, Gruszczyńska K, Baron J, Markowski J. Nasal region dimensions in children: a CT study and clinical implications. Biomed Res Int 2014;2014:125810.
34. Subtelny JD. A longitudinal study of soft tissue facial structures and their profile characteristics, defined in relation to underlying skeletal structures. Am J Orthod Dentofacial Orthop 1959;45(7):481–507.
35. van der Heijden P, Korsten-Meijer AG, van der Laan BF, Wit HP, Goorhuis-Brouwer SM. Nasal growth and maturation age in adolescents: a systematic review. Arch Otolaryngol Head Neck Surg 2008;134 (12):1288–93.
36. Macho GA. An appraisal of plastic reconstruction of the external nose. J Forensic Sci 1986;31(4):1391–403.